CHAPTER 8: Diffusion

Diffusion and ion implantation are the two key processes to introduce a controlled amount of dopants into semiconductors and to alter the conductivity type. ***Figure 8.1*** compares these two techniques and the resulting dopant profiles. In the diffusion process, the dopant atoms are introduced from the gas phase of by using doped-oxide sources. The doping concentration decreases monotonically from the surface, and the in-depth distribution of the dopant is determined mainly by the temperature and diffusion time. ***Figure 8.1b*** reveals the ion implantation process, which will be discussed in Chapter 9. Generally speaking, diffusion and ion implantation complement each other. For instance, diffusion is used to form a deep junction, such as an n-tub in a CMOS device, while ion implantation is utilized to form a shallow junction, like a source / drain junction of a MOSFET.

Boron is the most common p-type impurity in silicon, whereas arsenic and phosphorus are used extensively as n-type dopants. These three elements are highly soluble in silicon with solubilities exceeding 5×10^{20} atoms / cm^3 in the diffusion temperature range (between 800°C and 1200°C). These dopants can be introduced via several means, including solid sources (BN for B, As_2O_3 for As, and P_2O_5 for P), liquid sources (BBr_3, $AsCl_3$, and $POCl_3$), and gaseous sources (B_2H_6, AsH_3, and PH_3). Usually, the gaseous source is transported to the semiconductor surface by an inert gas (e.g. N_2) and is then reduced at the surface.

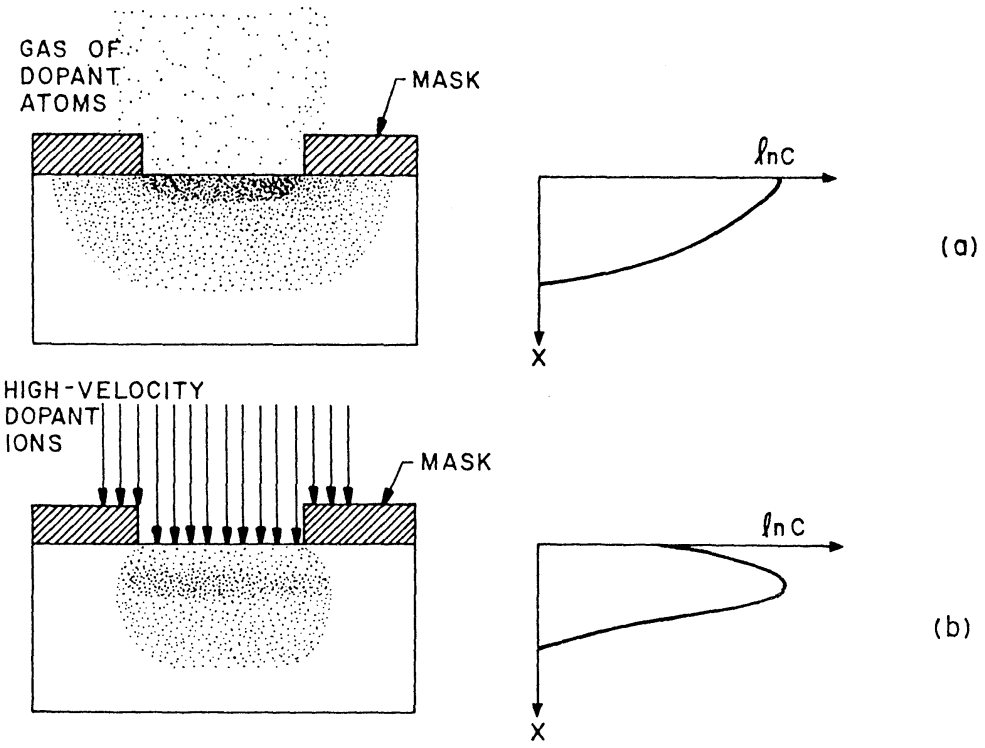

Figure 8.1: Comparison of (**a**) diffusion and (**b**) ion implantation for the selective introduction of dopants into a semiconductor substrate.

Chapter 8

8.1 Diffusion Theory

Diffusion in a semiconductor can be envisaged as a series of atomic movement of the diffusant (dopant) in the crystal lattice. ***Figure 8.2*** illustrates the two basic atomic diffusion mechanisms. The open circles represent the host atoms occupying the equilibrium lattice positions. The solid dots represent impurity atoms. At elevated temperature, the lattice atoms vibrate around the equilibrium lattice sites. There is a finite probability that a host atom can acquire sufficient energy to leave the lattice site and to become an interstitial atom thereby creating a vacancy. When a neighboring impurity migrates to the vacancy site, as shown in ***Figure 8.2a***, the mechanism is called vacancy diffusion. If an interstitial atom moves from one place to another without occupying a lattice site (***Figure 8.2b***), the mechanism is interstitial diffusion.

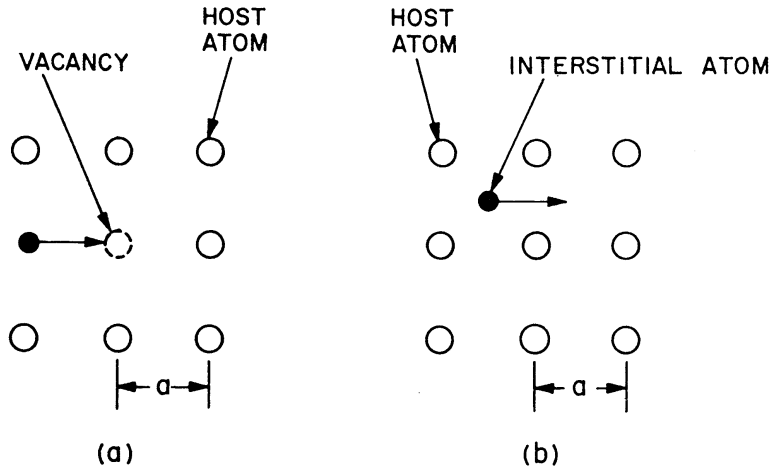

Figure 8.2: Models of atomic diffusion mechanisms for a two-dimensional lattice, with ***a*** being the lattice constant: (**a**) Vacancy mechanism. (**b**) Interstitial mechanism.

The basic diffusion process of impurity atoms is similar to that of charge carriers. Let F be the flux of dopant atoms traversing through a unit area in a unit time, and

$$F = -D\frac{\partial C}{\partial x} \qquad \textit{(Equation 8.1)}$$

where D is the diffusion coefficient, C is the dopant concentration, and x is the distance in one dimension. The equation imparts that the main driving force of

the diffusion process is the concentration gradient, $\frac{\partial C}{\partial x}$. In fact, the flux is proportional to the concentration gradient, and the dopant atoms will diffuse from a high-concentration region toward a low-concentration region. The negative sign on the right-hand-side of *Equation 8.1* states that matters flow in the direction of decreasing dopant concentration, that is, the concentration gradient is negative.

According to the law of conservation of matter, the change of the dopant concentration with time must be equivalent to the local decrease of the diffusion flux, in the absence of a source or a sink. Thus,

$$\frac{\partial C}{\partial t} = -\frac{\partial F}{\partial x} = \frac{\partial}{\partial x}(D\frac{\partial C}{\partial x}) \qquad \textit{(Equation 8.2)}$$

When the concentration of the dopant is low, the diffusion constant at a given temperature can be considered as a constant and *Equation 8.2* can be written as:

$$\frac{\partial C}{\partial t} = D\frac{\partial^2 C}{\partial x^2} \qquad \textit{(Equation 8.3)}$$

Equation 8.3 is often referred to as Fick's Second Law of Diffusion.

Figure 8.3 displays the measured diffusion coefficients for low concentrations of various dopant impurities in silicon and gallium arsenide. The logarithm of the diffusion coefficients plotted against the reciprocal of the absolute temperature yield a straight line in most of the cases, implying that over the temperature range, the diffusion coefficients can be expressed as:

$$D = D_o e^{-\frac{E_a}{kT}} \qquad \textit{(Equation 8.4)}$$

where D_o denotes the diffusion coefficient extrapolated to infinite temperature and E_a stands for the Arrhenius activation energy.

For interstitial diffusion, E_a is related to the energy required to move a dopant atom from one interstitial site to another. The values of E_a are between 0.5 to 1.5 eV in both Si and GaAs. For vacancy diffusion, E_a is related to both the energies of motion and formation of vacancies. Hence, E_a for vacancy diffusion is larger than that for interstitial diffusion and is usually between 3 to 5 eV. For fast diffusing species such as Cu, the measured activation energy is less than 2 eV, implying that interstitial atomic movement is the dominant diffusion mechanism.

For slow diffusing species like As, E_a is higher than 3 eV, and vacancy diffusion is naturally the dominant mechanism.

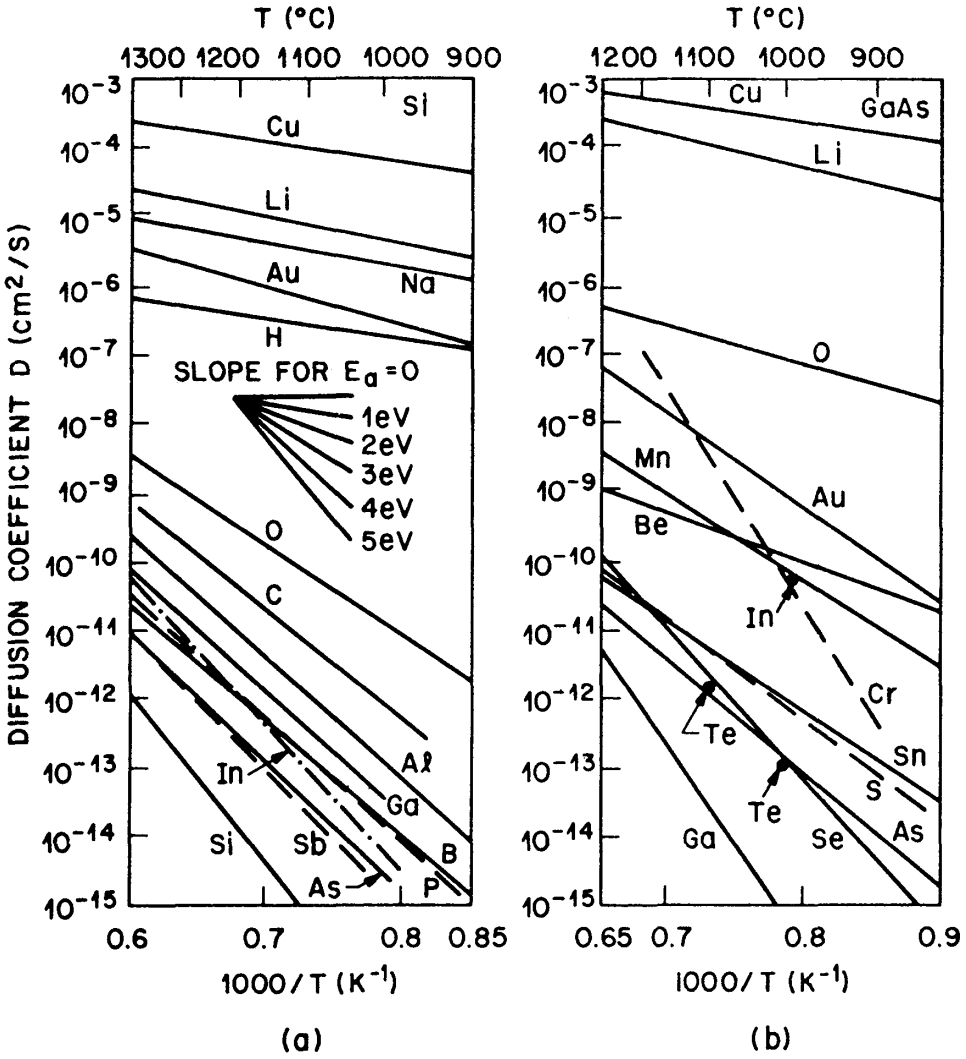

Figure 8.3: Diffusion coefficient (also called diffusivity) as a function of the reciprocal of temperature for (**a**) silicon and (**b**) gallium arsenide.

Chapter 8

8.2 Diffusion Profiles

The diffusion profile of dopant atoms is dependent on the initial and boundary conditions. Solutions for *Equation 8.3* have been obtained for various simple conditions, including constant-surface-concentration diffusion and constant-total-dopant diffusion. In the first scenario, impurity atoms are transported from a vapor source onto the semiconductor surface and diffuse into the semiconductor wafer. The vapor source maintains a constant level of surface concentration during the entire diffusion period. In the second situation, a fixed amount of dopant is deposited onto the semiconductor surface and is subsequently diffused into the wafer.

8.3 Constant-Surface-Concentration Diffusion

The initial condition at $t = 0$ is $C(x, 0) = 0$ which states that the dopant concentration in the host semiconductor is initially zero. The boundary conditions are:

$$C(0, t) = C_s \text{ and } C(\infty, t) = 0$$

where C_s is the surface concentration (at $x = 0$) which is independent of time. The second boundary condition states that at large distances from the surface, there are no impurity atoms. The solution of the differential equation that satisfies the initial and boundary conditions is given by:

$$C(x,t) = C_s erfc\left\{\frac{x}{2\sqrt{Dt}}\right\} \qquad \textit{(Equation 8.5)}$$

where *erfc* stands for the complementary error function, $\sqrt{Dt}$ is the diffusion length, x is the distance, D is the diffusion coefficient, and t is the diffusion time. Some properties of the erfc are summarized in ***Table 8.1***.

The diffusion profile for the constant-surface-concentration condition is exhibited in ***Figure 8.4(a)*** on both linear and logarithmic scales. The total number of dopants per unit area of the semiconductor, $Q(t)$, is given by integrating $C(x, t)$ from $x = 0$ to $x = \infty$:

$$Q(t) = \frac{2}{\sqrt{\pi}} C_s \sqrt{Dt} \cong (1.13) C_s \sqrt{Dt} \qquad \textit{(Equation 8.6)}$$

The gradient of the diffusion, $\frac{dC}{dx}$, can be obtained by differentiating *Equation 8.5*, and the result is:

$$\frac{dC}{dx} = -\frac{C_s}{\sqrt{\pi Dt}} \exp\left\{\frac{-x^2}{4Dt}\right\} \qquad \textit{(Equation 8.7)}$$

Table 8.1: Error Function Algebra.

$erf\,(x)$	$\equiv$	$\frac{2}{\sqrt{\pi}}\int_0^x e^{-y^2}\,dy$
$erfc\,(x)$	$\equiv$	$1 - erf(x)$
$erf\,(0)$	$=$	0
$erf\,(\infty)$	$=$	1
$erf\,(x)$	$\cong$	$\frac{2}{\sqrt{\pi}}x$ for $x << 1$
$erfc\,(x)$	$\cong$	$\frac{1}{\sqrt{\pi}}\frac{e^{-x^2}}{x}$ for $x >> 1$
$\frac{d}{dx}erf\,(x)$	$=$	$\frac{2}{\sqrt{\pi}}e^{-x^2}$
$\frac{d^2}{dx^2}\,erf\,(x)$	$=$	$-\frac{4}{\sqrt{\pi}}xe^{-x^2}$
$\int_0^x erfc(y')dy'$	$=$	$x\;\; erfc(x) \;+\; \frac{1}{\sqrt{\pi}}(1-e^{-x^2})$
$\int_0^\infty erfc(x)dx$	$=$	$\frac{1}{\sqrt{\pi}}$

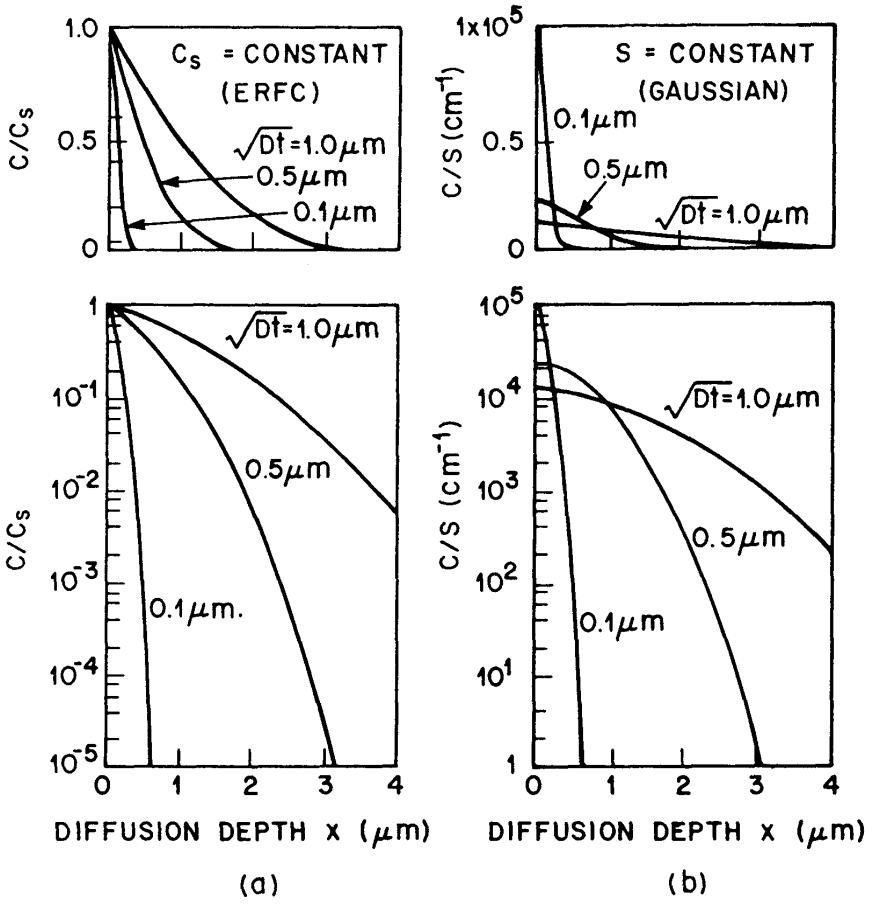

Figure 8.4: Diffusion profiles. (**a**) Normalized complementary error function (*erfc*) versus distance for successive diffusion times. (**b**) Normalized Gaussian function versus distance for successive times.

8.4 Constant-Total-Dopant Diffusion

For this case, a fixed (or constant) amount of dopant is deposited onto the semiconductor surface in a thin layer, and the dopant is subsequently diffused into the semiconductor. The initial condition at $t = 0$ is again $C(x, 0) = 0$. The boundary conditions are:

$$\int_0^\infty C(x,t)\ dx = S \quad and \quad C(\infty,t) = 0$$

where S is the total amount of dopant per unit area. The solution of the diffusion equation satisfying the above conditions is:

$$C(x,t) = \frac{S}{\sqrt{\pi Dt}} \exp\left\{\frac{-x^2}{4Dt}\right\} \qquad \textit{(Equation 8.8)}$$

This expression is the Gaussian distribution, and the dopant profile is displayed in *Figure 8.4b*. By substituting $x = 0$ into *Equation 8.8*:

$$C_s(t) = \frac{S}{\sqrt{\pi Dt}} \qquad \textit{(Equation 8.9)}$$

The dopant surface concentration therefore decreases with time, since the dopant will move into the semiconductor as time increases. The gradient of the diffusion profile is obtained by differentiating *Equation 8.8*:

$$\frac{dC}{dx} = -\frac{x}{2Dt} C(x,t) \qquad \textit{(Equation 8.10)}$$

The gradient is zero at $x = 0$ and $x = \infty$, and the maximum gradient occurs at $x = \sqrt{2Dt}$.

Both the complementary error function and the Gaussian distribution are functions of a normalized distance, $\frac{x}{2\sqrt{Dt}}$. Hence, if we normalize the dopant concentration with the surface concentration, each distribution can be represented by a single curve valid for all diffusion times, as shown in ***Figure 8.5***.

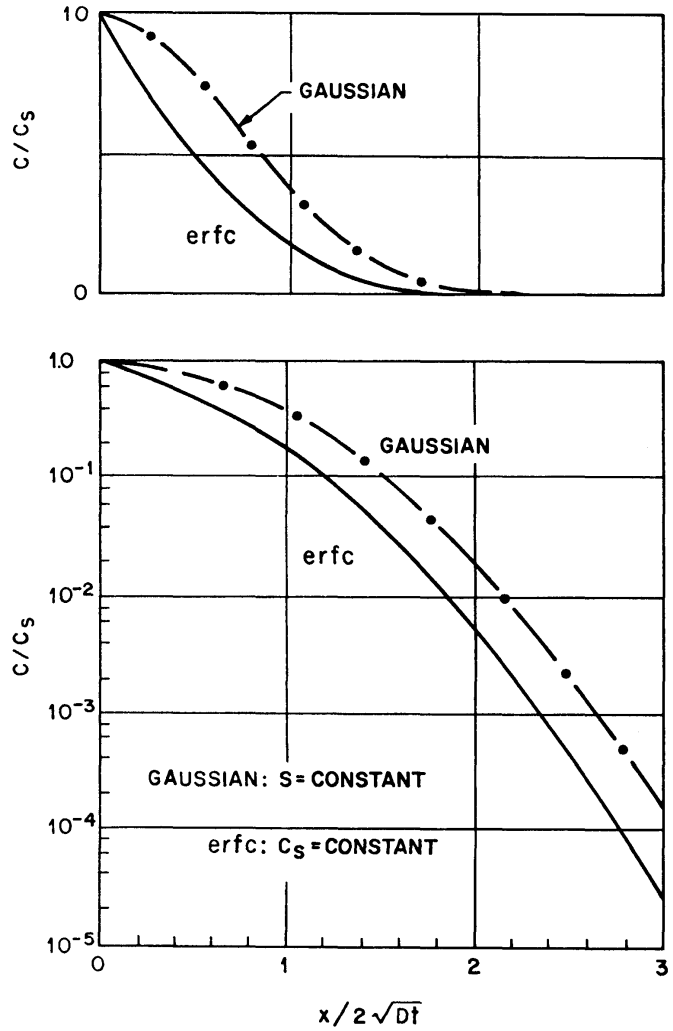

Figure 8.5: Normalized concentration versus normalized distance for the *erfc* and Gaussian functions.

Chapter 8

Example 8.1

Phosphorus is added to a silicon wafer from a gaseous source at 975°C for 30 minutes. Determine the junction depth for: (a) 0.3 Ω-cm p-type substrate and (b) 20 Ω-cm p-type substrate. Assume that the diffusion coefficient of phosphorus is 10^{-13} cm^2 s^{-1} and that its solid solubility is 10^{21} cm^{-3} at 975°C.

Solution

The diffusion mechanism is governed by the complementary error function:

$$C(x,t) = C_S erfc\left\{\frac{x}{2\sqrt{Dt}}\right\}$$

$C_S = 10^{21}$ cm^{-3}; $D = 10^{-13}$ cm^2 s^{-1} at 975°C

(a)

Resistivity = 0.3 Ω-cm p-type or $N_A = 6.3 \times 10^{16}$ cm^{-3} from ***Fig. 1.11***

$C / C_S = 6.3 \times 10^{16} / 10^{21} = 6.3 \times 10^{-5}$

$\frac{x}{2\sqrt{Dt}}$ = 2.83 from ***Fig. 8.5***

$x_j = (2.83)(2)[(10^{-13})(1800)]^{1/2} = 7.6 \times 10^{-5}$ cm = 0.76 μm

(b)

Resistivity = 20 Ω-cm p-type or $N_A = 6.8 \times 10^{14}$ cm^{-3} from ***Fig. 1.11***

$C / C_S = 6.8 \times 10^{14} / 10^{21} = 6.8 \times 10^{-7}$

$\frac{x}{2\sqrt{Dt}}$ = 3.5 from ***Fig. 8.5*** (Extending the erfc line linearly on a log scale is reasonable in this range)

$x_j = (3.5)(2)[(10^{-13})(1800)]^{1/2} = 9.4 \times 10^{-5}$ cm = 0.94 μm

Chapter 8

8.5 Dual Diffusion Process

In VLSI processing, a two-step diffusion sequence is commonly used, in which a predeposition diffusion layer is formed under a constant-surface-concentration condition and is followed by a drive-in diffusion or redistribution under a constant-total-dopant condition. For most practical cases, the diffusion length $\sqrt{Dt}$ for the predeposition diffusion is much smaller than that for the drive-in condition. Hence, the predeposition profile can be treated as a delta function at the surface.

Chapter 8

Example 8.2

(a) A predeposition process is carried out for 15 minutes on an *n*-type silicon wafer with a phosphorus dopant concentration of 10^{17} atoms/cm^3 at 950^{o}C using diborane gas. Assuming intrinsic diffusion, determine the junction depth. At 950^{o}C the boron saturation concentration is 3.8 x 10^{20} atoms/cm^3 and the boron diffusion constant is 1.5 x 10^{-15} cm^2/s.

(b) After the initial predeposition process described in (a), the sample undergoes a drive-in diffusion for 1 hour at 1250^{o}C. What is the final junction depth? At 1250^{o}C, the boron diffusion constant is 1.2 x 10^{-12} cm^2/s.

Solution

(a)

The junction depth is determined by the point of transition from *p*-type to *n*-type silicon. For a predeposition process, the diffusion behavior is given by the complementary error function. Therefore, the junction depth, x_j, is determined by:

$$C(x_j,t) = C_s erfc\left\{\frac{x_j}{2\sqrt{Dt}}\right\} = 10^{17}$$

$$erfc\left\{\frac{x_j}{2\sqrt{Dt}}\right\} = \frac{10^{17}}{3.8x10^{20}} = 2.63x10^{-4}$$

From ***Fig. 8.5***, for $\frac{c}{c_s} = 2.63x10^{-4}$, $\frac{x}{2\sqrt{Dt}} = 2.6$

Thus, $x_j = 2.6x2x\sqrt{(1.5x10^{-15})(900)} = 6.04x10^{-6}$ cm or 0.06 μm.

(b)

The total integrated dose, *S*, in the predeposition process is:

$$S = \frac{2}{\sqrt{\pi}} C_s \sqrt{Dt} = \frac{2}{1.77}(3.8x10^{20})\sqrt{(1.5x10^{-15})(900)} = 5x10^{14}$$

Since the drive-in time and temperature (D_{1250C} >> D_{950C}) is much larger than those in the predeposition process, the boron distribution resulting from the predeposition can be assumed to be a delta function. For the drive-in process, the dopant profile is given by the Gaussian distribution:

$$C(x,t) = \frac{S}{\sqrt{\pi Dt}} \exp\left\{\frac{-x^2}{4Dt}\right\}.$$

Thus, $10^{17} = \frac{5x10^{14}}{\sqrt{\pi(1.2x10^{-12})(3600)}} \exp\left\{\frac{-x_j^{\,2}}{4(1.2x10^{-12})(3600)}\right\}$

$$10^{17} = 4.3x10^{18} \exp\left\{\frac{-x_j^{\,2}}{1.7x10^{-8}}\right\}$$

$$2.3x10^{-2} = \exp\left\{\frac{-x_j^{\,2}}{1.7x10^{-8}}\right\}$$

$$-3.76 = \frac{-x_j^{\,2}}{1.7x10^{-8}}$$

Thus, x_j = 2.5 x 10^{-4} cm or 2.5 μm.

Example 8.3

(a) A predeposition process is carried out for 15 minutes on an *n*-type silicon wafer with a bulk doping concentration of 10^{17} atoms/cm^3 at 950°C using diborane gas. Determine the *p-n* junction depth given that the surface solubility of boron at 950°C is 3.8 x 10^{20} atoms/cm^3, the intrinsic diffusivity (D_o) is 0.76 cm^2/s, and the Arrhenius activation energy (E_a) is 3.46 eV.

(b) A drive-in process is subsequently performed on this sample after the deposition process. In order to produce a *p-n* junction 1.28 μm below the wafer surface, estimate the required *Dt*, the product of the diffusion coefficient and time. Based on your result, determine the time required if the drive-in temperature is 1250°C.

Solution

(a)

Using *Equation 8.4*,

$$D = 0.76e^{-\frac{3,46}{(8.36x10^{-5})(1223)}} = 1.527x10^{-15}\ \text{cm}^2/\text{s}$$

For the predeposition, the distribution is given by the erfc function.

C_s = 3.8x10^{20} atoms/cm^3

At the junction depth, C = 10^{17} atoms/cm^3

Therefore, $\frac{C}{C_s} = \frac{10^{17}}{3.8x10^{20}} = 2.63x10^{-4}$

Using the erfc curve in ***Fig. 8.5***, the corresponding value of $\frac{x}{2\sqrt{Dt}}$ is 2.58.

Thus, $\frac{x_j}{2\sqrt{Dt}} = 2.58 = \frac{x_j}{2\sqrt{(1.527x10^{-15})(15x60)}}$.

The junction depth, x_j = 6.05x10^{-6} cm = 0.0605 μm.

Chapter 8

(b)

The drive-in process yields the Gaussian distribution and the amount of dopant introduced during the predeposition process is given by *Equation 8.6*:

$$Q = (1.13)C_s\sqrt{Dt} = (1.13)(3.8x10^{20})\sqrt{(1.527x10^{-15})(15x60)} = 5.03x10^{14}\ \text{cm}^{-2}$$

Substituting this value of Q or S into *Equation 8.8*,

$$C(x_j,t) = \frac{S}{\sqrt{\pi Dt}}\exp\left\{-\frac{x_j^{\,2}}{4Dt}\right\} = \frac{5.03x10^{14}}{\sqrt{\pi Dt}}\exp\left\{-\frac{1.28x10^{-4}}{4Dt}\right\} = 10^{17}$$

Using trial and error gives $Dt = 9 \times 10^{-9}$ cm^2

$$D = 0.76e^{-\frac{3,46}{(8.36x10^{-5})(1523)}} = 1.193x10^{-12}.$$

Hence, $t = \dfrac{9x10^{-9}}{D} = 7.54x10^{3}$ seconds or 126 minutes.

8.6 Extrinsic Diffusion

Diffusion that occurs when the doping concentration is lower than the intrinsic carrier concentration, n_i, at the diffusion temperature is called intrinsic diffusion. In this region, the resulting dopant profiles of sequential or simultaneous diffusion of n-type or p-type impurities can be determined by superposition, that is, the diffusion processes can be treated independently. However, when the dopant concentration exceeds n_i (e.g. at 1000°C, n_i = 5 x 10^{18} atoms/cm^3), the process becomes extrinsic, and the diffusion coefficients become concentration dependent, as shown in ***Figure 8.6***.

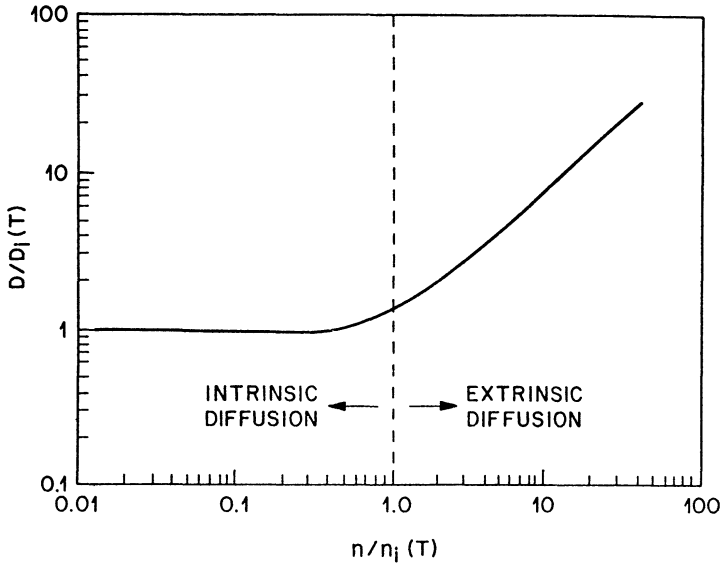

Figure 8.6: Donor impurity diffusion coefficient versus electron concentration showing regions of intrinsic and extrinsic diffusion.

When a host atom acquires sufficient energy and leaves its lattice site, a vacancy is created. Depending on the charges associated with the vacancy, we can have:
(1) a neutral vacancy, V^o,
(2) an acceptor vacancy, V^-,
(3) a doubly-charged acceptor vacancy, V^{2-},
(4) a donor vacancy, V^+,
(5) and others.

The vacancy density of a given charge state (i.e., the number of vacancies per unit volume) has a temperature dependence similar to that of the carrier density:

$$C_v = C_i e^{\frac{E_F - E_i}{kT}} \qquad \textit{(Equation 8.11)}$$

where C_v is the vacancy density, C_i is the intrinsic vacancy density, E_F is the Fermi level, and E_i is the intrinsic Fermi level.

If the dopant diffusion is dominated by the vacancy mechanism, the diffusion coefficient is expected to be proportional to the vacancy density. At low doping concentrations ($n < n_i$), the Fermi level coincides with the intrinsic Fermi level (i.e., $E_F = E_i$). The vacancy density is equal to C_i and independent of the dopant concentration. The diffusion coefficient, which is proportional to C_i, will also be independent of doping concentration. At high doping concentrations ($n > n_i$), the Fermi level will move toward the conduction band edge for donor-type vacancies, and the term $e^{\frac{E_F - E_i}{kT}}$ becomes larger than unity. This causes C_v to increase, which in turn gives rise to enhanced diffusion, as exhibited in *Figure 8.6*.

When the diffusion coefficient varies with the dopant concentration, we should use *Equation 8.2* in lieu of *Equation 8.3*. We shall also consider the situation where the diffusion coefficient can be written as:

$$D = D_s\left(\frac{C}{C_s}\right)^{\gamma} \qquad \textit{(Equation 8.12)}$$

where D_s is the diffusion coefficient at the surface, C_s is the surface concentration, and γ is a positive integer. Therefore,

$$\frac{\partial C}{\partial t} = \frac{\partial}{\partial x}\left(D_s\left\{\frac{C}{C_s}\right\}^{\gamma}\frac{\partial C}{\partial x}\right) \qquad \textit{(Equation 8.13)}$$

Equation 8.13 can be solved numerically, and the solutions for constant-surface-concentration diffusion are shown in ***Figure 8.7***, along with the result for a constant D (i.e., $\gamma = 0$). For concentration-dependent diffusion, the diffusion profiles are much steeper at low concentrations ($C << C_S$). Thus, highly abrupt junctions can be formed when diffusion is made into a background of an opposite impurity type. In fact, the abruptness of the doping profile results in a junction depth is virtually independent of the background concentration.

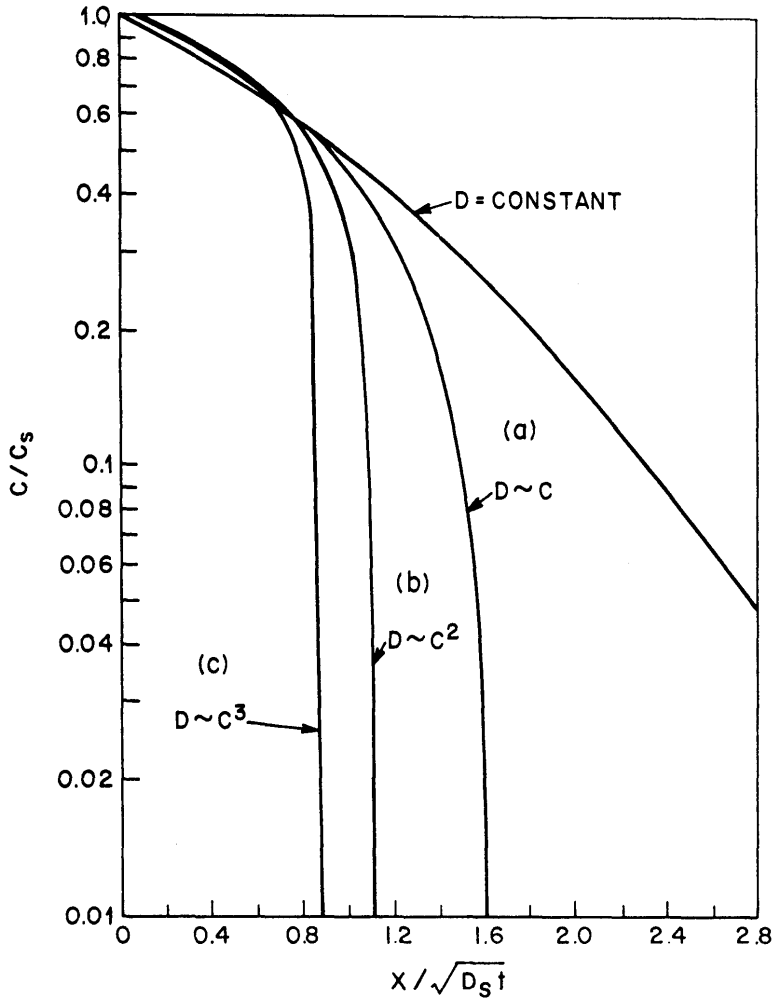

Figure 8.7: Normalized diffusion profiles for extrinsic diffusion where the diffusion coefficient becomes concentration dependent.

8.7 Diffusion in Silicon

The measured diffusion coefficients of arsenic and phosphorus as a function of dopant concentration are displayed in ***Figure 8.8***. The diffusion of arsenic in silicon is associated with the acceptor-type vacancy, V^-, and the diffusion coefficient for $n > n_i$ can be written as:

$$D = D_o^{'}(\frac{n}{n_i})e^{-\frac{E_a^{'}}{kT}} \qquad \textit{(Equation 8.14)}$$

where $D_o^{'}$ = 45.8 cm^2/s, $E_a^{'}$ = 4.05 eV, and n is the carrier concentration (or dopant concentration, assuming 100% activation). The junction depth is essentially independent of the indigenous p-type concentration, and is given by:

$$x_j = 1.6\sqrt{D_s t} = 1.6\left\{\left(D_o^{'}e^{-\frac{E_a^{'}}{kT}}\right)\left(\frac{C_s}{n_i}t\right)\right\}^{1/2} \qquad \textit{(Equation 8.15)}$$

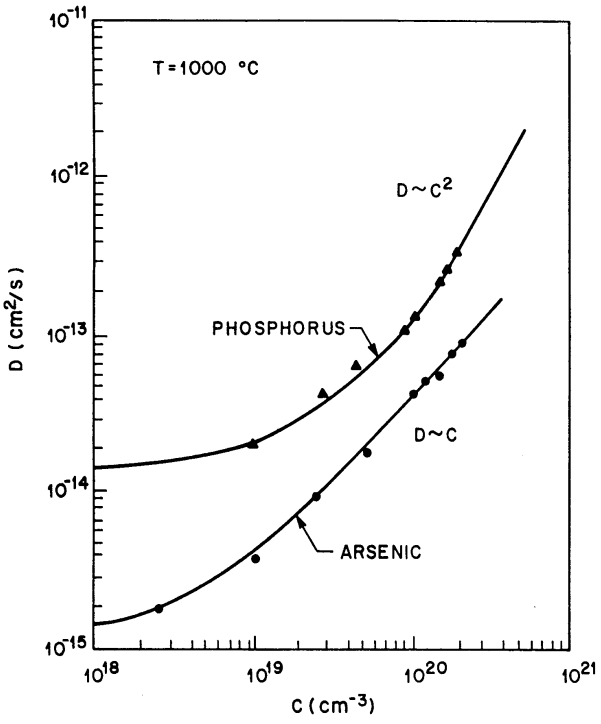

Figure 8.8: Extrinsic diffusivities of arsenic and phosphorus in silicon as a function of dopant concentration.

The measured diffusion profile for arsenic is shown as curve (a) in ***Figure 8.9*** where Y_j is equal to $\frac{x_j}{\sqrt{4D_s t}}$ and x_j is given by *Equation 8.15*. Owing to its abrupt doping profile, arsenic is used extensively to form shallow junctions such as the source and drain regions in n-channel MOSFETs.

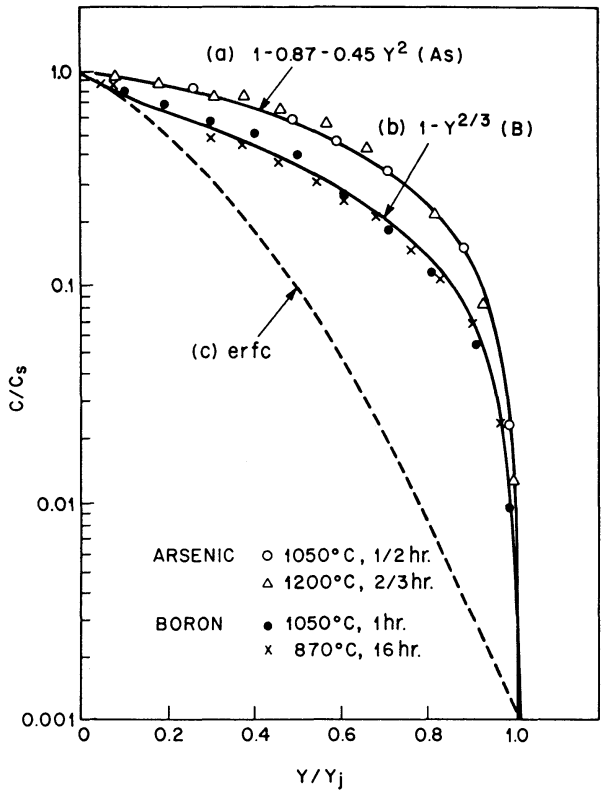

Figure 8.9: Normalized diffusion profiles for arsenic and boron in silicon. The *erfc* distribution is shown for comparison.

The diffusion of boron in silicon is associated with donor-type vacancy, V^+, and the diffusion coefficient varies approximately linearly with dopant concentration. The expression for D has the same form as *Equation 8.14*, except that D_o' is 1.52 cm^2/s, E_a' is 3.46 eV and n is replaced by p. The measured boron profile is exhibited as curve (b) in ***Figure 8.9*** and is less abrupt than the arsenic profile. Note that both the boron and arsenic profiles are steeper than the erfc case shown as curve (c) in ***Figure 8.9***.

The diffusion of phosphorus in silicon is associated with the doubly-charged acceptor vacancy, V^{2-}, and the diffusion coefficient at high concentrations varies as C^2 (***Figure 8.8***). ***Figure 8.10*** depicts the phosphorus diffusion profiles into

silicon for 1 hour at 1000°C. When the surface concentration is low (i.e., intrinsic diffusion region), the diffusion profile is given by the *erfc* [curve (a)]. As the concentration increases, the profile begins to deviate from the simple expression [curves (b) and (c)]. At a very high concentration [curve (d)], the profile near the surface is indeed similar to that shown as curve (b) in ***Figure 8.7***. However, at concentration n_e, a kink occurs followed by a rapid diffusion (broader in-depth distribution) in the tail region. The concentration n_e corresponds to a Fermi level 0.11 eV below the conduction band. At this energy level, the coupled impurity-vacancy pair (P^+V^{2-}) dissociates to P^+, V^-, and an electron. A large number of singly-charged acceptor vacancies V^- are generated to enhance diffusion in the tail region of the profile. The diffusivity in the tail region is over 10^{-12} cm^2/s, which is about 2 orders of magnitude larger than the intrinsic diffusivity at 1000°C. Therefore, phosphorus is commonly used to form deep junctions such as n-tubs in a CMOS device.

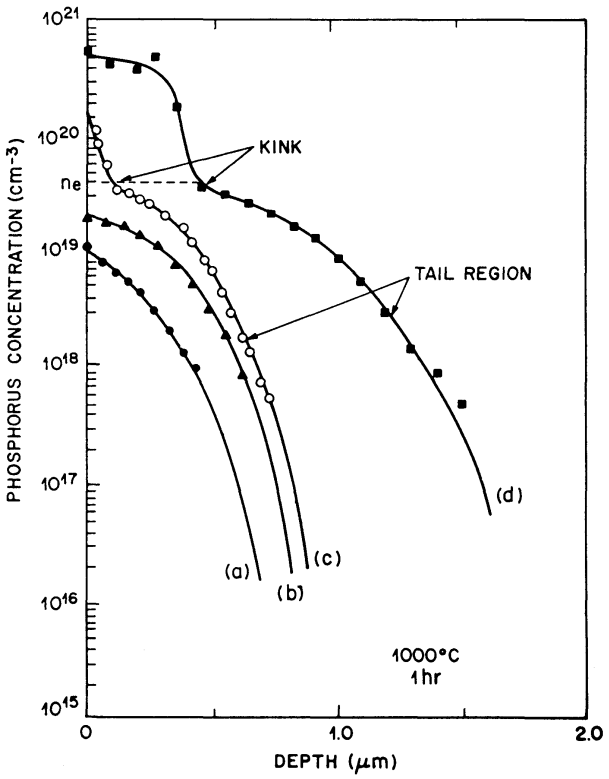

Figure 8.10: Phosphorus diffusion profiles for various surface concentrations after diffusion into silicon for 1 hour at 1000°C.

8.8 Emitter Push Effect

In silicon n-p-n bipolar transistors employing a phosphorus-diffused emitter and a boron-diffused base, the base region under the emitter region (inner base) is deeper by up to 0.6 μm than that outside the emitter region (outer base). This phenomenon is called the emitter push effect, as illustrated in ***Figure 8.11***. The dissociation of phosphorus vacancy (P^+V^{2-}) pairs at the kink region provides a mechanism for the enhanced diffusion of phosphorus in the tail region. The diffusivity of boron under the emitter region (inner base) is also enhanced by the dissociation of P^+V^{2-} pairs.

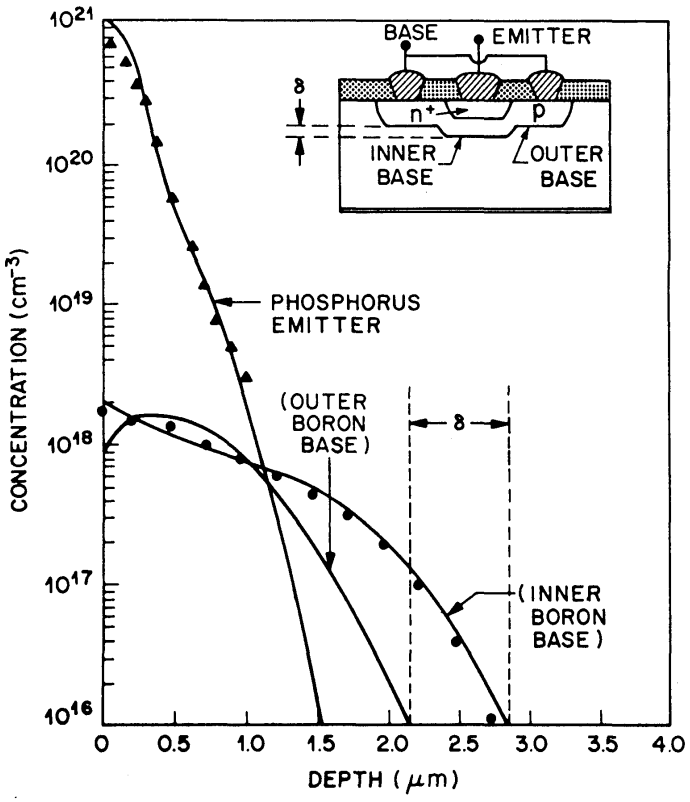

Figure 8.11: Calculated and measured boron and phosphorus n-p-n transistor profile showing the emitter push effect. Emitter diffusion is at 1000°C for 1 hour followed by a 900°C, 45-minute steam oxidation.

8.9 Measurement Techniques

The results of a diffusion process can be evaluated by three parameters:
(1) Junction depth.
(2) Sheet resistance.
(3) Dopant profile.

8.9.1 Staining

Junction depths are commonly measured on an angle-lapped (1^o to 5^o) sample chemically stained by a mixture of 100 c.c. HF (49%) and a few drops of HNO_3. If the sample is subjected to strong illumination for one to two minutes, the p-type region will be stained darker than the n-type region, as a result of a reflectivity difference of the two etched surfaces. The location of the stained junction depends on the p-type concentration level and sometimes on the concentration gradient. In general, the stain boundary corresponds to a concentration level in the range of mid-10^{17} atoms/cm^3.

Alternatively, junction depths can be delineated by cutting a groove into the semiconductor and etching the surface (***Figure 8.12***). If R_o is the radius of the tool used to form the groove, the junction depth, x_j, is given by:

$$x_j = (a^2 - b^2) / 2R_o \qquad \textit{(Equation 8.17)}$$

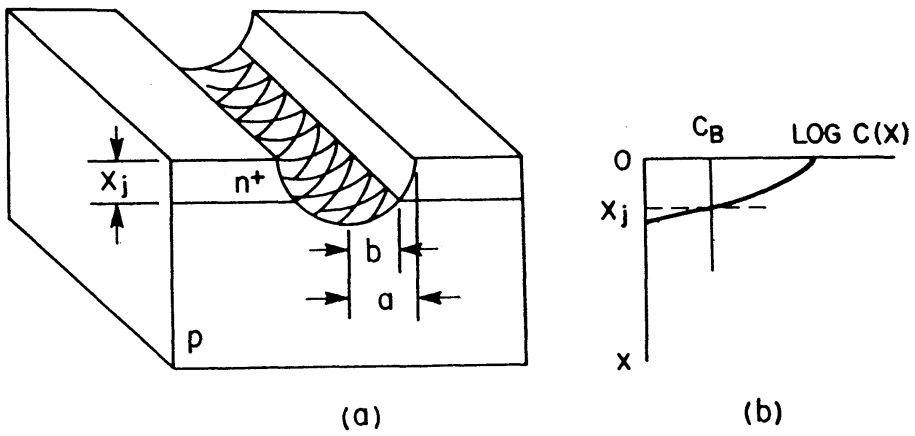

Figure 8.12: Junction depth measurement by grooving and staining.

8.9.2 Four-Point Probe

The sheet resistivity of a diffused layer can be measured by a four point probe:

$$R_s = \frac{V}{I}[C.F.] \qquad \textit{(Equation 8.18)}$$

where R_s is the sheet resistance, V is the measured voltage across the voltage probes, I is the constant dc current passing through the current probes, and *C. F.* is the correction factor to account for differences in sample size, geometry, and probe positions.

8.9.3 Spreading Resistance Profiling

In spreading resistance profiling (SRP), two probes are used. The total spreading resistance, R_{sr}, is given by:

$$R_{sr} = \rho / 2a \qquad \textit{(Equation 8.20)}$$

where ρ is the average resistivity near the probe points and a is the probe radius. If the two probes are stepped simultaneously in discrete intervals along a beveled edge as illustrated in ***Figure 8.13***, a high depth resolution profile of the electrical carrier concentration can be acquired.

8.9.4 Secondary Ion Mass Spectrometry

Secondary ion mass spectrometry (SIMS) is very useful in elucidating impurity diffusion profiles with excellent depth resolution (1 nm – 20 nm) and high sensitivity ("parts per million" to "parts per billion" detection limits). An oxygen or cesium ion beam of energy 1 to 20 keV is used to sputter a sample and the sputtered ions are separated according to their mass-to-charge ratios (m/e) by a mass spectrometer typically composed of a magnetic sector or quadrupole. SIMS provides elemental (atomic) information whereas electrical techniques such as spreading resistance profiling reveal electrical carrier concentration. If a dopant is 100% activated (ionized), the SIMS and SRP results should theoretically agree.

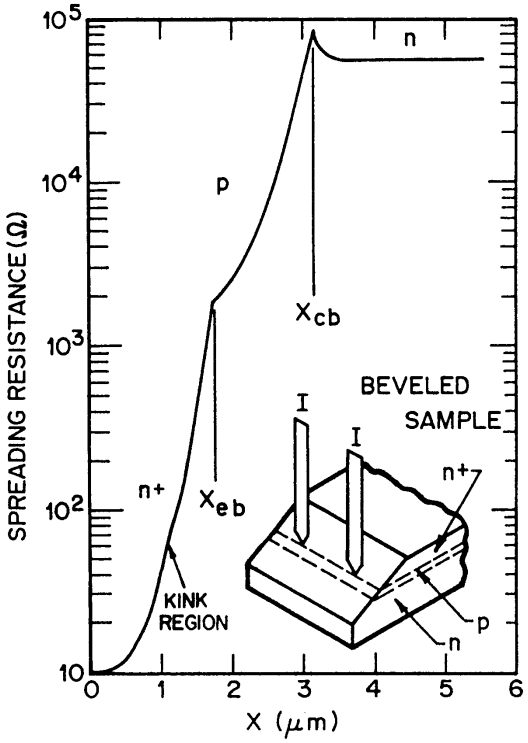

Figure 8.13: The spreading resistance profile of an npn transistor structure: x_{eb} = emitter – base junction depth = 1.7 μm; x_{cb} = collector – base junction depth = 3.2 μm.

8.10 Oxide Masking

The diffusivities of common dopants are considerably smaller in silicon dioxide than in silicon. Therefore, silicon dioxide is an effective mask against impurities. The diffusion process in SiO_2 occurs in two steps. During the first step, the dopant reacts with silicon dioxide to form a glass that grows until the entire silicon dioxide film is consumed (forming PSG, for instance). After the glass forms, the dopant diffuses into the silicon substrate. Hence, during the first step, silicon dioxide is completely effective in masking the silicon substrate against dopants in the gas phase. The thickness of silicon dioxide required for an effective masking is determined by the rate of formation of the glass, which in turn is governed by the diffusion of the impurity into the silicon dioxide. ***Figure 8.14*** shows the minimum thickness, *d*, of dry-oxygen-grown silicon dioxide required to mask against phosphorus and boron as a function of temperature and time. For a given temperature, *d* varies as $\sqrt{t}$, as the diffusion length is given by $\sqrt{Dt}$.

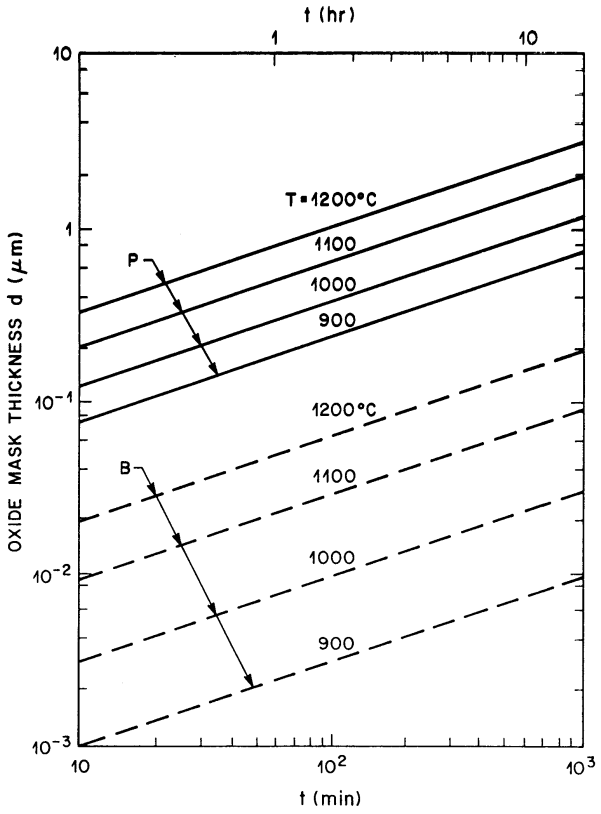

Figure 8.14: Minimum thickness of dry-oxygen-grown SiO_2 required to mask against phosphorus and boron as a function of diffusion time with the diffusion temperature as a parameter.

8.11 Lateral Diffusion

The one-dimensional diffusion equation discussed previously cannot adequately describe the process at the edge of the mask window, at which the impurities will diffuse both downward and laterally. In this case, a two-dimensional diffusion equation must be used and solved numerically. ***Figure 8.15*** depicts the contours for constant-surface-concentration diffusion assuming that the diffusivity is independent of concentration. As shown, the vertical penetration is about 2.8 μm, whereas the lateral one is about 2.3 μm. The lateral penetration is thus about 80% of the vertical penetration. In the case of constant-total-dopant diffusion, this ratio is about 70%. For concentration-dependent diffusivities, this ratio is reduced slightly to about 65% to 70%.

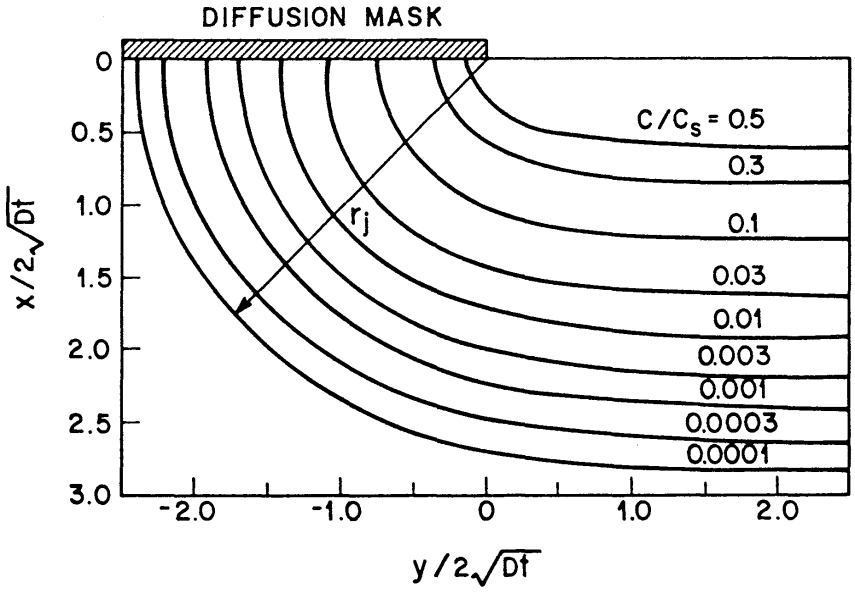

Figure 8.15: Diffusion contours at the edge of an oxide window, where r_j is the radius of curvature.

Chapter 8

8.12 Fast Diffusants

Some elements are fast diffusants in silicon. They include the groups I and VII elements, and some heavy metals, such as Au, Cu, Pt, and so on. They are therefore undesirable contaminants in VLSI and are usually gettered away from the active device regions by internal gettering techniques, that is, using SiO_x clusters in the bulk of the wafer to trap impurities.

Chapter 8

8.13 Diffusion in Polysilicon

Polysilicon films are typically used in VLSI as a gate or as an intermediate conductor in two-level systems. Since the gate electrode is over a thin oxide (15 nm to 150 nm thick), it is imperative that dopant atoms in the polysilicon do not diffuse through the gate oxide. Polysilicon films are usually deposited at a low temperature without doping elements. After the gate region is defined, the polysilicon film is doped by diffusion (from a doped-oxide source or gas source) or by ion implantation.

Impurity diffusion in polysilicon film can be explained qualitatively by a grain-boundary model. A polysilicon film is composed of single crystallites of varying sizes that are separated by grain boundaries. The diffusivity of impurity atoms that migrate along grain boundaries can be up to 100 times larger than that in a single crystal lattice. In addition, experimental results indicate that impurity atoms inside each crystallite have diffusivities either comparable to or a factor of 10 larger than those found in the single crystal. The diffusivity in a polysilicon film therefore depends strongly upon the structure (grain size, etc.) and texture. These are in turn functions of the film deposition temperature, rate of deposition, thickness, and composition of the substrate. Hence, it is difficult to predict diffusion profiles in polysilicon. Diffusivities are typically estimated from junction depths and surface concentrations are determined experimentally.